The Astrophysical Journal, 646:1230–1240, 2006 August 1

WHOLE EARTH TELESCOPE OBSERVATIONS OF THE PULSATING SUBDWARF B STAR PG 0014+067

M. Vučković,[1,2] S. D. Kawaler,[1] S. O'Toole,[3] Z. Csubry,[4] A. Baran,[5] S. Zola,[5,6] P. Moskalik,[7] E. W. Klumpe,[8] R. Riddle,[9] M. S. O'Brien,[10] F. Mullally,[11] M. A. Wood,[12] V. Wilkat,[12] A.-Y. Zhou,[13] M. D. Reed,[13] D. M. Terndrup,[14] D. J. Sullivan,[15] S.-L. Kim,[16] W. P. Chen,[17] C.-W. Chen,[17] W.-S. Hsiao,[17] K. Sanchawala,[17] H.-T. Lee,[17] X. J. Jiang,[18] R. Janulis,[19,20] M. Siwak,[6] W. Ogloza,[5] M. Paparó,[4] Zs. Bognár,[4] Á. Sódor,[4] G. Handler,[21] D. Lorenz,[21] B. Steininger,[21] R. Silvotti,[22] G. Vauclair,[23] R. Oreiro,[24] R. Østensen,[25] A. Bronowska,[25] B. G. Castanheira,[26] S. O. Kepler,[26] L. Fraga,[27] H. L. Shipman,[28] J. L. Provencal,[28] and D. Childers[28]

Received 2006 February 22; accepted 2006 April 13

ABSTRACT

PG 0014+067 is one of the most promising pulsating subdwarf B stars for seismic analysis, as it has a rich pulsation spectrum. The richness of its pulsations, however, poses a fundamental challenge to understanding the pulsations of these stars, as the mode density is too complex to be explained only with radial and nonradial low-degree ($l < 3$) p-modes without rotational splittings. One proposed solution, suggested by Brassard et al. in 2001 for the case of PG 0014+067 in particular, assigns some modes with high degree ($l = 3$). On the other hand, theoretical models of sdB stars suggest that they may retain rapidly rotating cores, and so the high mode density may result from the presence of a few rotationally split triplet ($l = 1$) and quintuplet ($l = 2$) modes, along with radial ($l = 0$) p-modes. To examine alternative theoretical models for these stars, we need better frequency resolution and denser longitude coverage. Therefore, we observed this star with the Whole Earth Telescope for two weeks in 2004 October. In this paper we report the results of Whole Earth Telescope observations of the pulsating subdwarf B star PG 0014+067. We find that the frequencies seen in PG 0014+067 do not appear to fit any theoretical model currently available; however, we find a simple empirical relation that is able to match all of the well-determined frequencies in this star.

Subject headings: stars: individual (PG 0014+067) — stars: oscillations — subdwarfs

Online material: color figures

1. INTRODUCTION

Even though stellar evolution is one of the most mature areas in theoretical astrophysics, there are still phases in the life of an ordinary star (like our Sun) that are not well understood. We have a nearly continuous evolutionary path of a low massive star all the way from its birthplace, a protostellar cloud, to its graveyard, with few gaps in our understanding. However, at least one major gap remains, the core helium flash that initiates helium core burning. Unlike most phases of stellar evolution, the flash itself occurs in a matter of minutes rather than millions of years. It is essentially a massive runaway nuclear reaction near the center of the star that releases a huge amount of energy on a short timescale. Despite ignition on a dynamical timescale, apparently this event does not make the star explode, because we *do* see stars that are clearly survivors of this process. Post-helium-core-flash objects are identified with horizontal branch stars in globular clusters and their field counterparts.

[1] Department of Physics and Astronomy, 12 Physics Hall, Iowa State University, Ames, IA 50011.
[2] Instituut voor Sterrenkunde, Celestijnenlaan 200B, 3001 Leuven, Belgium.
[3] Dr. Remeis-Sternwarte, Astronomisches Institut der Universität Erlangen-Nürnberg, Sternwartstrasse 7, Bamberg 96049, Germany.
[4] Konkoly Observatory, P.O. Box 67, H-1525 Budapest XII, Hungary.
[5] Mount Suhora Observatory, Cracow Pedagogical University, Ul. Podchorazych 2, 30-084 Krakow, Poland.
[6] Astronomical Observatory, Jagiellonian University, Ul. Orla 171, 30-244 Krakow, Poland.
[7] Nicolas Copernicus Astronomical Center, Polish Academy of Sciences, Ul. Bartycka 18, 00-716 Warsaw, Poland.
[8] Department of Physics and Astronomy, Middle Tennessee State University, Murfreesboro, TN 37132.
[9] California Institute of Technology, Pasadena, CA 91125.
[10] Department of Astronomy, Yale University, New Haven, CT 06851.
[11] Department of Astronomy, University of Texas, Austin, TX 78712.
[12] Department of Physics and Space Sciences and SARA Observatory, Florida Institute of Technology, Melbourne, FL 32901.
[13] Department of Physics, Astronomy and Material Science, Missouri State University, Springfield, MO 65897.
[14] Department of Astronomy, Ohio State University, Columbus, OH 43210.
[15] Department of Physics, Victoria University of Wellington, P.O. Box 600, Wellington, New Zealand.
[16] Korea Astronomy and Space Science Institute, Daejeon 305-348, South Korea.
[17] Institute of Astronomy, National Central University Taiwan, 32054 ChungLi, Taiwan.
[18] National Astronomical Observatories, Chinese Academy of Sciences, Beijing 100012, China.
[19] Institute of Theoretical Physics and Astronomy, Goštauto 12, Vilnius 2600, Lithuania.
[20] Astronomical Observatory of Vilnius University, Čiurlionio 29, Vilnius 2009, Lithuania.
[21] Institut für Astronomie, Türkenschanzstrasse 17, A-1180 Vienna, Austria.
[22] INAF-Osservatorio Astronomico di Capodimonte, via Moiariello 16, I-80131 Naples, Italy.
[23] Université Paul Sabatier, Observatoire Midi-Pyrénées, 14 Avenue E. Belin, 31400 Toulouse, France.
[24] Departamento de Física Aplicada, Universidad de Vigo, Vigo 36200, Spain.
[25] Isaac Newton Group of Telescopes, Santa Cruz de La Palma 37800, Canary Islands, Spain.
[26] Instituto de Física, Universidade Federal de Rio Grande do Sul, 91501-900 Porto-Alegre, RS, Brazil.
[27] Departamento de Física, Universidade Federal de Santa Catarina, Florianópolis, Brazil.
[28] Department of Physics and Astronomy, University of Delaware, 223 Sharp Laboratory, Newark, DE 19716.

At the extreme blue end of the horizontal branch, subdwarf B (sdB) stars are survivors of the core helium flash that have a small hydrogen-rich envelope surrounding the helium-burning core. According to evolutionary calculations, for example, those by Dorman et al. (1993), sdB stars are core helium-burning stars with a canonical mass of $M \approx 0.5\ M_{\odot}$ and a very thin, inert hydrogen envelope with $M_{\rm H}/M_{*} \sim 0.0004$, which places them on the hot end of the horizontal branch, the so-called extreme horizontal branch. The fact that sdB stars have lost almost all of their hydrogen layer is what makes them so enigmatic from the stellar evolution point of view. To lose that much mass, they must suffer a considerable mass loss during the red giant branch and most probably during the helium core flash.

Details of the origin of the sdB stars are largely unknown. There are currently many competing theories for their origin, which involve several possible channels. These include single-star evolution with an extreme mass loss on the red giant branch (D'Cruz et al. 1996), or different binary interactions: common-envelope binary evolution (Mengel et al. 1976), stable Roche lobe overflow (Han et al. 2002, 2003 and references therein), or merging of two helium white dwarfs (Iben 1990).

The most fundamental missing piece to our understanding of the evolution of the sdB stars is the nature and physics behind their mass loss (Fusi Pecci & Renzini 1976). To end up on the extreme horizontal branch they must lose nearly all of their hydrogen at almost exactly the same phase as the helium core has attained the minimum mass required for the helium flash to occur. By exposing the interior properties of these survivors, we can learn how the stars manage to survive this event of unstable helium ignition and plug this gap in the story of stellar evolution.

Luckily, some of these stars pulsate, letting us, therefore, use the tools and techniques of asteroseismology to probe their interiors. Discovered by Kilkenny et al. (1997), the pulsating sdB stars (officially designated V361 Hya stars but also called sdBV stars by analogy with the pulsating white dwarfs) are short-period, low-amplitude multimode pulsators. Typical periods are about 100–250 s with an overall period range of 80–600 s. The pulsation amplitudes are generally less than a few hundredths of a magnitude. The short periods, being of the order of and shorter than the radial fundamental mode for these stars, suggest that the observed modes are low-order, low-degree $p-$modes (Charpinet et al. 2000).

The rapidly pulsating sdB stars occupy a region in the $\log g$-$T_{\rm eff}$ plane with effective temperatures of $T_{\rm eff} = 29{,}000$–$36{,}000$ K and surface gravities $\log g = 5.2$–6.5. Many of the high-gravity pulsating sdB stars show complex pulsations that require a large number of modes. Radial modes alone are not enough to explain the complex light curves of these stars; therefore, nonradial modes must also be present (Kawaler 1999; Kilkenny et al. 1999; Charpinet et al. 2000).

Among the sdBV stars PG 0014+067 stands out as one of the richest pulsators. It was found to be an sdBV star in 1998 June (Brassard et al. 2001). While close binaries like KPD 1930+2752 (Poindexter et al. 2003) and lower gravity sdB pulsators like PG 1605+072 (Kilkenny et al. 1999) can show dozens of modes, PG 0014+067 is a higher gravity, single sdB star that shows a large number of nonradial modes, with at least 16 reported in the discovery paper. Periods range from 80 to 170 s. It is a "typical" sdBV star with an effective temperature of $T_{\rm eff} = 33{,}310$ K and $\log g = 5.8$ (Brassard et al. 2001). The richness of its pulsation, however, makes it a star of vital interest to the study of sdBV stars and, by extension, the entire hot horizontal branch phenomenon. The rich mode density in PG 0014+067 poses a fundamental challenge to understanding the pulsations of these stars, as there are not enough radial and nonradial modes with low degree l ($l < 3$) to account for all of them (without rotational splitting). Low-degree nonradial modes have a limited frequency distribution, which implies that we need to resort to higher values of l to account for all of the observed periodicities. That presents further challenges, as geometrical cancellation increases rapidly with l so that higher l modes need to have a much larger intrinsic amplitude than low-l modes to reach the same observable amplitude.

One solution, proposed Brassard et al. (2001), presents an envelope structural model that approximates their determined pulsation frequencies with p-modes of degrees 0, 1, 2, and 3. Their resulting seismic model provides an estimate of the mass of PG 0014+067 of $0.49 \pm 0.02\ M_{\odot}$ and, in addition, matches the observed spectroscopic parameters and places strict limits on the thickness of the surface hydrogen layer.

Another possible explanation for the mode density in PG 0014+067 comes from theoretical calculations of the evolution of stars on the red giant branch, and the subsequent structure on the horizontal branch. These models show that stars can develop a rapidly rotating core on the red giant branch and then preserve that core on the horizontal branch. If that is the case, then certain modes of pulsation in sdBV stars could show large rotational splitting, much larger than suggested by the (slow) surface rotation velocity. Models by Kawaler & Hostler (2005) in particular point out that rotational splittings of low-order $l = 1$ and 2 modes can cause sufficient frequency peaks in the observed range provided that the stellar core rotates much faster than its surface. These models show rotational splitting that can vary by factors of 2 or more from one mode to the next. If that is the case in PG 0014+067, then it could sufficiently complicate the observed mode spectrum with modes of $l = 0$, 1, and 2 alone.

The only published observations of PG 0014+067 are single-site data from Brassard et al. (2001) who have observed this star using the 3.6 m Canada-France-Hawaii Telescope (CFHT) during five consecutive nights (1.9 hr average run length) in 1998 June. These data show that the oscillation spectrum is complex, but being single-site data, they suffer from severe 1 cycle per day aliases, making the frequency identification rather difficult.

To fully exploit this star we need to determine, unambiguously, the oscillation frequencies present. This can be achieved only by extended longitude coverage with a sufficient frequency resolution to be able to resolve the real pulsations from the inevitable 1 cycle per day aliases. With a secure set of oscillation frequencies, we can critically examine the proposed theoretical models for these stars without concern for fitting artifacts caused by diurnal aliasing instead of true oscillation modes. PG 0014+067 was selected as the primary target for a Whole Earth Telescope (WET) campaign, held in 2004 October. In this paper we present the results of this multisite campaign. In § 2 we present the observations followed by a review of the data reduction procedure. In § 3 we report on the frequency analysis of the WET data set on PG 0014+067, and we discuss the results in § 4 along with the plans for future work.

2. OBSERVATIONS

PG 0014+067 was a primary target during the 24th WET run, Xcov24, held in 2004. Being a faint star, with $V \approx 16.5$, and a low-amplitude pulsator—most modes have amplitudes below 2 mmag—we sought larger-than-average ($\geq$2 m class) telescopes distributed around the Earth. Time was allocated to five such telescopes (>2 m) that were well distributed in longitude. Observations spanned two weeks centered around new moon from 2004 October 7 to 21. With a right ascension near 0 hr, and a

TABLE 1
JOURNAL OF OBSERVATIONS OF PG 0014+067 IN 2004 OCTOBER

Run Name	Telescope	UT Date	Start (UT)	Duration (hr)	Instrument
mdr275[a]	MDM 1.3 m	05	08:55:15	2.10	CCD
teide-10072004[a]	Tenerife 0.8 m	08	02:36:40	0.55	CCD
sara213	SARA 0.9 m	08	02:47:59	8.74	CCD
PG0014_08oct04	Loiano 1.5 m	08	19:24:50	5.50	CCD
sara214	SARA 0.9 m	09	01:58:59	9.20	CCD
PG0014_09oct04[a]	Loiano 1.5 m	09	19:45:09	1.44	CCD
PG0014_10oct04	Loiano 1.5 m	10	19:09:20	6.35	CCD
lulin-0001	Lulin 1.0 m	11	11:10:35	8.35	CCD
041012A	NAOC 2.16 m	12	12:27:00	7.50	PMT
korea-001	BOAO 1.8 m	12	13:02:10	5.45	CCD
korea-002	BOAO 1.8 m	13	10:19:20	5.32	CCD
041013A[a]	NAOC 2.16 m	13	11:27:22	8.50	PMT
lit-01	Moletai 1.56 m	13	21:49:20	4.65	PMT
france-01[a]	Pic Du Midi 2.0 m	13	20:50:00	2.85	PMT
041014A	NAOC 2.16 m	14	11:23:30	8.49	PMT
korea-003	BOAO 1.8 m	14	10:55:16	7.27	CCD
lit-05	Moletai 1.56 m	14	19:00:10	7.37	PMT
korea-004	BOAO 1.8 m	15	10:19:00	7.75	CCD
A0934	McDonald 2.1 m	15	06:26:07	2.65	CCD
NOT-001	NOT 2.6 m	15	19:55:23	4.32	CCD
NOT-002	NOT 2.6 m	16	00:19:52	4.87	CCD
lulin-0008	Lulin 1.0 m	16	12:34:26	6.45	CCD
NOT-003	NOT 2.6 m	16	19:43:22	8.37	CCD
rkb1[a]	LNA 1.6 m	17	02:25:04	3.15	CCD
A0939	McDonald 2.1 m	17	05:19:58	1.04	CCD
A0940[a]	McDonald 2.1 m	17	07:32:18	1.32	CCD
lulin-0010	Lulin 1.0 m	17	11:36:36	7.51	CCD
maja10182004	KPNO 2.1 m	18	09:06:40	1.78	CCD
lulin-0012	Lulin 1.0 m	18	10:50:02	3.10	CCD
041018B	NAOC 2.16 m	18	13:47:00	5.88	PMT
maja10192004	KPNO 2.1 m	19	05:19:40	3.40	CCD
lulin-0015	Lulin 1.0 m	19	10:43:11	8.33	CCD
maja10202004	KPNO 2.1 m	20	02:11:20	3.18	CCD
maja10202004b	KPNO 2.1 m	20	09:39:40	0.93	CCD
lulin-0016	Lulin 1.0 m	20	11:35:48	7.35	CCD
hungary-007[a]	Konkoly 1.0 m	20	18:09:56	1.56	CCD

[a] Runs not used because of low signal-to-noise ratio.

near-equatorial declination of +7°, PG 0014+067 was equally accessible from both Northern and Southern Hemisphere sites during this time of the year. As a contingency, smaller telescopes (<2 m) with CCD detectors were included to minimize the gaps in the data and to simplify the alias pattern of our spectral window. Together with 13 smaller telescopes, 18 sites participated in this campaign.

Unluckily, nonphotometric conditions all over the globe during the main campaign resulted in less-than-ideal coverage. Table 1 lists all the observations gathered during Xcov24 on PG 0014+067. As can be noticed from the log of the observations given in Table 1, much of the data did not come from our bigger telescopes (>2 m) because of the bad weather conditions, but from moderate-size ones (between 1 and 2 m). The 1.0 m telescope at Lulin Observatory in Taiwan contributed data on six nights. An additional four nights of high-quality data came from the Bohyunsan Optical Astronomy Observatory (BOAO) 1.8 m telescope in South Korea. Surprisingly good data were also obtained by the Southeastern Association for Research in Astronomy (SARA) 0.9 m telescope at Kitt Peak National Observatory (KPNO), given the relatively small size of the telescope. Despite the terrible weather and some unexpected instrumental problems we had during Xcov24, the 2 week core campaign resulted in about 180 hr of data on the primary target, yielding a duty cycle of about 58%. The WET run on PG 0014+067 spans 2 weeks, which results in a formal frequency resolution of $\Delta\nu = 0.9$ μHz.

The telescopes used for the primary target range in aperture from 0.9 to 2.56 m. Data from National Astronomical Observatories, Chinese Academy of Sciences (NAOC), Moletai Observatory (Lithuania), and Pic Du Midi (France) were obtained using three-channel photomultiplier tubes (PMTs) as described by Kleinman et al. (1996). Exposure times were 5 s for 2 m telescopes (China and France) and 10 s for the 1.65 m telescope in Lithuania. Channel 1 measured the program star, channel 2 measured a local comparison star, and channel 3 simultaneously recorded sky background. All PMT photometric observations were taken in white light to maximize the photon count rate.

All other data were obtained using CCDs (see last column of Table 1). For the CCD measurements exposures ranged from 5 to 15 s, depending on the size of the telescope. As the readout times differ from chip to chip and were quite long for some sites, observations were made in the "windowed" mode, i.e., only a portion of the chip was read out to minimize the cycle time, making sure there were always at least two comparison stars in the frame. Observations from McDonald Observatory and Laboratório Nacional de Astrofísica (LNA) were made in the frame transfer

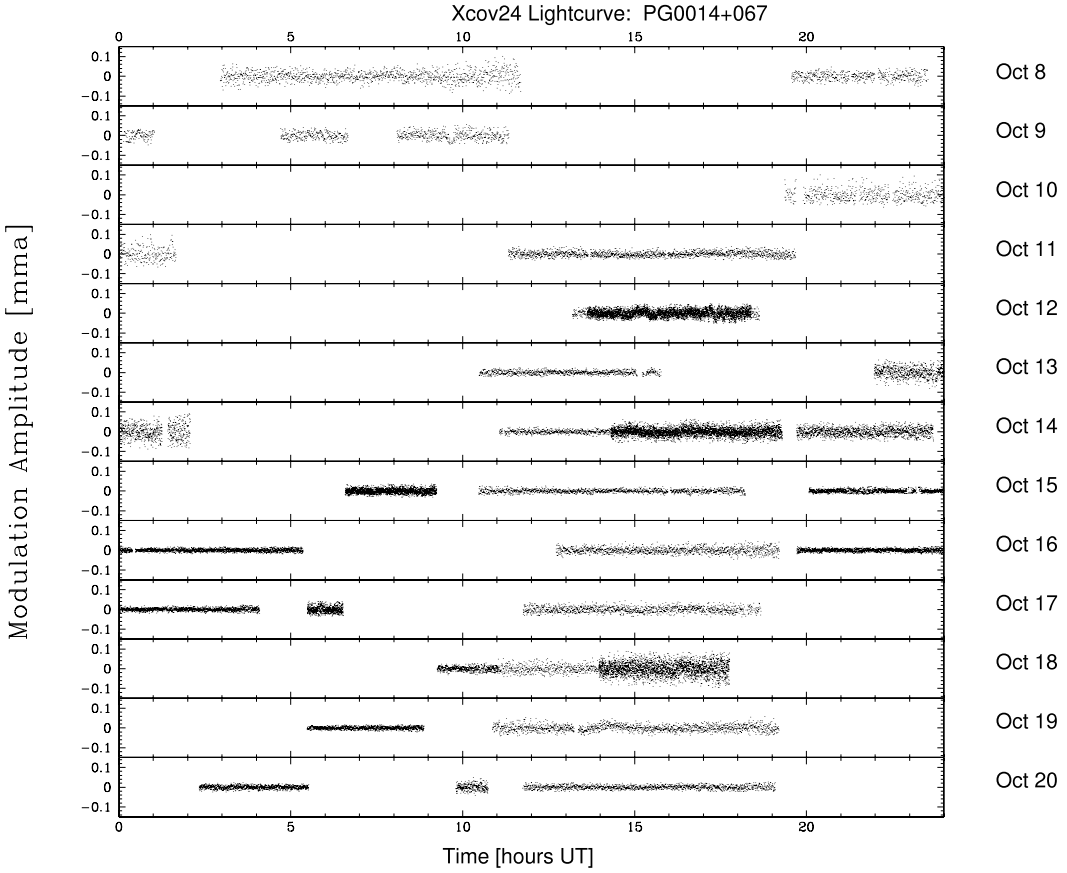

FIG. 1.—Light curve of PG 0014+067 obtained during Xcov24. Each panel spans 24 hr on the UT date indicated. Different density of data points comes from several factors: overlapping of the data, different sampling time, and different signal-to-noise ratio.

mode. The actual CCD frames at every individual site were never bigger than $5' \times 5'$ centered around the target. The number of comparison stars depended on the size of this window, having from two to six comparison stars in the frame. In this way consecutive data points were obtained in 5–25 s intervals, depending on the instrument. Data from McDonald and KPNO used BG 40 filters, and data from Nordic Optical Telescope (NOT) used a W92 filter. Together with the science frames, each night of observation included calibration images (bias, dark, and flat-field frames).

Preliminary, "on the fly" data reduction was done during the campaign at a central headquarters (Iowa State University). Since the WET collaboration does not operate with a standard CCD photometry extraction package, raw CCD frames were prereduced (overscan, bias, dark, flat-field corrected) by the observers using their own software immediately after the run, and the first-look photometry was sent to the headquarters (HQ) in the standard WET/XQED format. Incoming data were further reduced at HQ using the WET software XQED (Riddle 2003). These preliminary reductions were used during the course of the run to allocate telescopes between the primary target and secondary targets, and for preliminary analysis of the pulsation spectrum of PG 0014+067. For this paper, all the data were carefully rereduced by the lead author from the original CCD frames.

For the PMT data, reduction followed standard WET procedures. After the proper dead-time correction, the sky background (channel 3) was subtracted both from the target and from the comparison star point by point. When necessary, the variable star data were then divided by the comparison star to correct for transparency variations. To correct for any low-frequency variations caused by seeing and differential color extinction, the resulting light curve was then fitted with a low-order polynomial. Bad points, coming from either electronic noise, guiding errors, or clouds, were removed by hand. Finally, the light curve was mean subtracted, leaving only the fractional variations from the mean modulation amplitude (ma $= \Delta I/\langle I \rangle$), and a barycentric correction to the exposure midtimes was applied, giving the times of the data points projected to the barycenter of the solar system.

For our final reduction, the raw CCD data were reduced using the IRAF `ccdproc` package, and the reduction comprised correction for bias, dark counts and flat field. Further photometric measurements (aperture photometry) on these reduced frames were made using the `phot` package. After carefully examining the extracted aperture photometry for a set of different apertures for each observation, the aperture that gave the best signal-to-noise ratio was used. The apertures that typically gave the optimal signal-to-noise ratio in the resulting light curve had a radius of $\approx$1.75 times the FWHM, with the surrounding annulus to determine the local sky level. In this way each star in the frame has its own corresponding sky channel. The aperture photometry measurements derived in this way were then imported into XQED. The resulting light curves, showing a fractional variation of the intensity of light as a function of time are presented in Figure 1.

3. THE FREQUENCIES OF PG 0014+067

Combining all the light curves described in the previous section (Fig. 1), we computed the Fourier transform (FT) to deduce the periodicities present in the data. To optimize the number of detected intrinsic frequencies present in the total light curve, gathered with the different aperture telescopes (from 0.9 to 2.56 m), we weighted the data using the weighting scheme favored by Handler

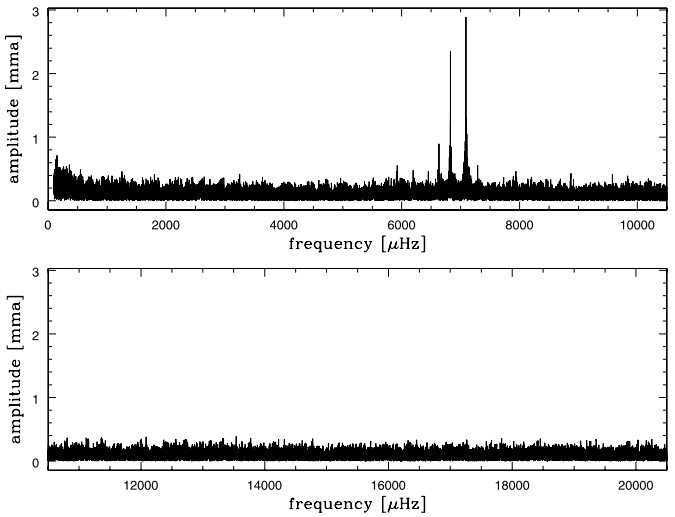

FIG. 2.—Weighted Fourier transform (amplitude spectrum) of the complete WET data set on PG 0014+067.

(2003). Weights are determined for individual runs, with the weight for a run taken as inversely proportional to the mean point-to-point scatter within the run. However, to some degree weighting inflates the amplitude of the daily aliases and widens the peaks. Consequently, weighting may affect the ability to resolve closely spaced peaks. Bearing this in mind, weighted data were used to expose and identify periodicities, but the frequencies, amplitudes, and phases of the individual peaks were determined using the "unweighted" data. The weighted FT of the full data set on PG 0014+067 gathered during Xcov24 is depicted in Figure 2 showing the modulation amplitude in units of mma = ma/1000, where ma = $\Delta I/I$, of variations in the detected intensity I at a given frequency.

To see the effect weighting has on the amplitude spectrum, we have calculated the spectral window for the weighted and unweighted data. Figure 3 shows the spectral window of the whole WET run on PG 0014+067 in both cases. The central peak in the

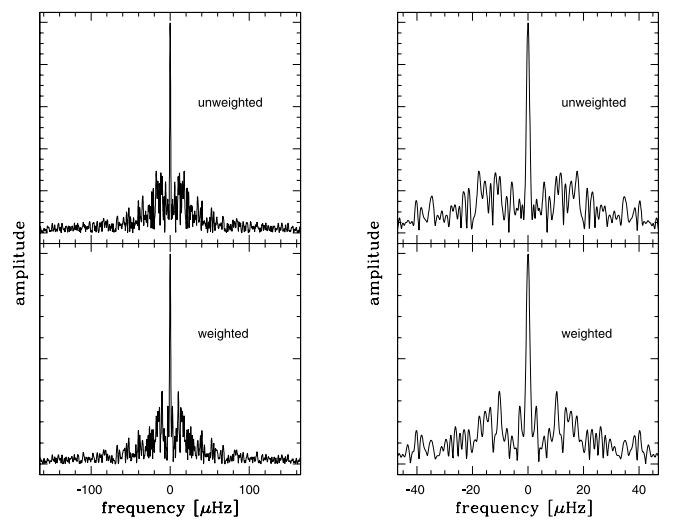

FIG. 3.—Spectral window for the PG 0014+067 WET data set. The expanded frequency range on the left displays the impact of the data sampling on the noise well beyond the 1 day^{-1}, while the closer view on the right shows the details of the alias pattern. Both cases (*top and bottom*) sample a noise-free sinusoid; the weights for the data were applied to the sinusoid to compute the window patterns shown in the bottom panels. The vertical amplitude scale is amplitude (in arbitrary units).

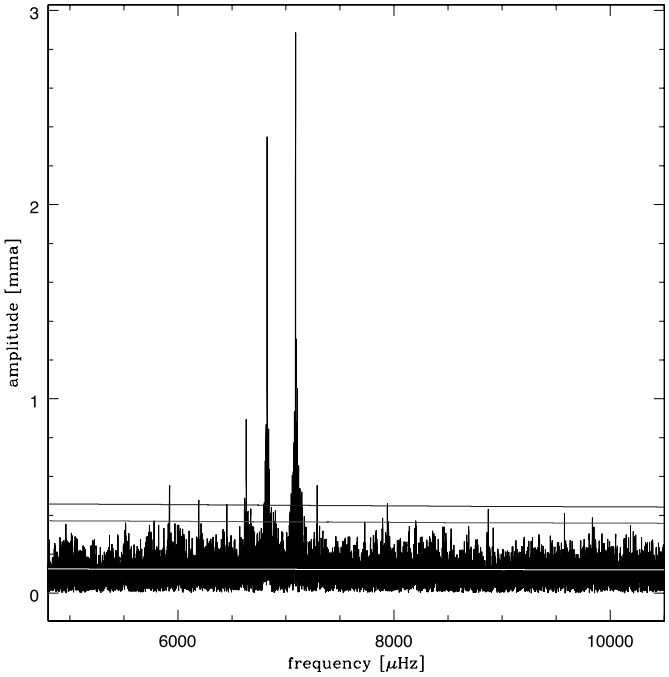

FIG. 4.—Weighted FT of the PG 0014+067 WET data expanded to the region of the most power. The mean noise level ($\sigma_{\rm noise}$), 3 $\sigma_{\rm noise}$, and 3.7 $\sigma_{\rm noise}$ are shown as nearly horizontal lines (*bottom to top, respectively*). [*See the electronic edition of the Journal for a color version of this figure.*]

plot corresponds to the input frequency of a single sinusoid; all other peaks are aliases caused by the gaps in the data set.

3.1. *Frequencies Found in the Xcov24 Data*

As can be clearly seen in Figure 2, the main action is concentrated in a very narrow frequency range. It appears as if all the power is distributed into two to three modes around the 7000 μHz with maximum intensity variations of $\sim$3 mma. This is a typical signature of a low-amplitude sdB pulsator (Kilkenny 2002). Figure 2 confirms that there are no frequencies with amplitudes above the mean noise level at higher frequencies, up to the Nyquist frequency ($f_{\rm N} \approx 30{,}000$ μHz). Therefore, we can securely focus our analysis on the narrow region of the main power. The spectral region above 20,000 μHz is not plotted, as it contains no additional information.

Figure 4 expands the FT of the entire data set around the region of the main power, 5000–10,000 μHz. The solid white line in Figure 4 corresponds to the noise level, $\sigma_{\rm noise}$; the corresponding middle line represents 3 times the noise level, 3 $\sigma_{\rm noise}$; while the top line represents 3.7 times the noise level, 3.7 $\sigma_{\rm noise}$. The noise in the power spectrum is calculated by averaging the amplitudes around each frequency in a wide frequency range. For our criterion determining which peaks are "real" signals in the power spectrum, we adopt a conservative significance threshold at 3.7 $\sigma_{\rm noise}$. Kuschnig et al. (1997) estimate that this results in a 99% confidence limit. The 3 $\sigma_{\rm noise}$ threshold is adopted by others as sufficient (Brassard et al. 2001; Metcalfe et al. 2005; Charpinet et al. 2005), which would correspond to an 80% confidence limit (Kuschnig et al. 1997). Hence, for comparison we show this lower threshold line in the figures.

Although the amplitude spectrum (Fig. 2) does not appear very complex, attempts to determine the underlying variations by prewhitening reveal that this star indeed has a complicated pulsation spectrum. After identifying the highest amplitude peak in the (computed) weighted power spectrum of the original data

TABLE 2
PERIODICITIES FOUND IN WET DATA ON PG 0014+067

Mode	Frequency (μHz)	Period (s)	Amplitude (mma)	T_{max}[a] (s)
f_7.....	5923.4 ± 0.1	168.821 ± 0.003	0.54 ± 0.13	20 ± 16
f_{10}.....	6193.5 ± 0.2	161.458 ± 0.005	0.44 ± 0.13	125 ± 20
f_9.....	6452.9 ± 0.2	154.968 ± 0.005	0.45 ± 0.13	150 ± 18
f_8.....	6631.9 ± 0.2	150.786 ± 0.005	0.49 ± 0.15	90 ± 20
f_6.....	6632.8 ± 0.1	150.766 ± 0.003	0.65 ± 0.15	143 ± 15
f_2.....	6826.06 ± 0.03	146.4974 ± 0.0006	2.38 ± 0.13	28 ± 3
f_1.....	7088.67 ± 0.03	141.0702 ± 0.0006	2.98 ± 0.13	8 ± 3
f_3.....	7091.0 ± 0.1	141.023 ± 0.002	1.22 ± 0.33	133 ± 11
f_4.....	7091.7 ± 0.1	141.011 ± 0.002	1.10 ± 0.32	55 ± 11
f_5.....	7289.0 ± 0.1	137.193 ± 0.002	0.65 ± 0.13	107 ± 11

[a] Time of first maximum after $T_0 = 2004$ August 21, 0 hr (UT).

set, we went back to the unweighted FT to confirm the periodicity. We then removed this peak from the data by subtracting a sine wave with the frequency, amplitude, and phase determined by nonlinear least-squares fit (NLLS) from the light curve. In our NLLS fits we use T_{max}, the time of first maximum after $T_0 =$ 2004 August 21 0 hr (UT), for the phase variable. We calculate the power spectrum of the residuals (light curve of the entire data set with this sinusoid removed). Then we looked at this prewhitened weighted FT to find the next highest peak and repeated the procedure. We determined the values of frequencies step by step, carefully checking whether new frequencies affected the other values and calculating a simultaneous n-frequency fit to the data until no new peaks could be identified with significance (with amplitude above 3.7 σ_{noise}). The results of this procedure are summarized in Table 2 and described in detail here.

Figure 5 illustrates this procedure. It shows the spectral window centered at 7000 μHz in the top panel, and the FT of the

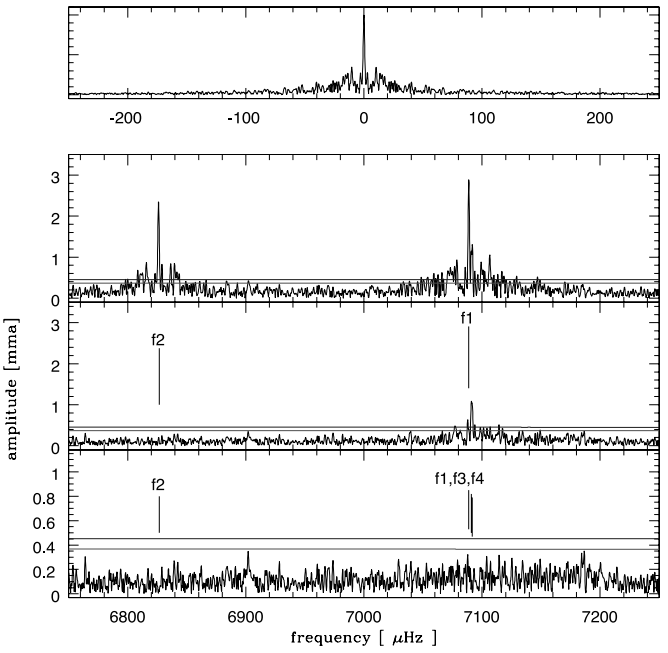

FIG. 5.—*Top:* Spectral window centered at 7000 μHz given on the same frequency scale as the data. *Second:* FT of the entire WET data set on PG 0014+067 expanded around the region of the highest power. *Third*: Residual FT prewhitened by f_1 and f_2 at frequencies indicated. *Bottom*: Prewhitened FT by the first four frequencies from Table 2. Note the different amplitude scale. [*See the electronic edition of the Journal for a color version of this figure.*]

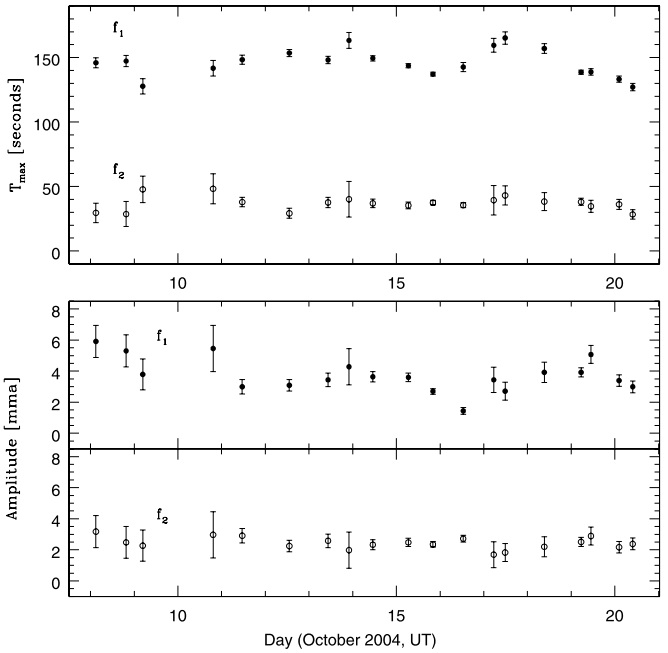

FIG. 6.—*Top:* Phase (T_{max}, in seconds) as a function of time for the two principal oscillations in PG 0014+067. Open circles are for f_2 and filled circles are for f_1. *Bottom:* Amplitude (in mma) for f_1 and f_2 over the course of the WET run.

entire data set in the region around the highest amplitude peaks in the second panel. The FT, prewhitened by the two highest peaks, $f_1 = 7088.67$ μHz with an amplitude of 3.0 mma and $f_2 =$ 6826.06 μHz with an amplitude of 2.4 mma, is presented at the third panel from the top of Figure 5. The highest amplitude peak f_1 appears to have fine structure, since significant power remains above the 3.7 σ_{noise} level (*top solid line*) after removing the highest peak at 7088.67 μHz. Two additional closely spaced peaks are present at frequencies $f_3 = 7091.0$ μHz and $f_4 = 7091.7$ μHz with amplitudes of 1.2 and 1.1 mma, respectively. Even though this frequency difference is formally unresolvable given our frequency resolution of 0.9 μHz, both of these modes are easily resolved in our NLLS fit to the data. Furthermore, all the power above the 3 σ_{noise} level (*lower solid line*) is gone after prewhitening the data with those three peaks (Fig. 5, *bottom*). The peak at 6826.06 μHz is cleanly removed by a single frequency prewhitening step.

In the extended observations of sdBV stars, it has been detected that the individual pulsation frequencies have amplitudes that vary in time. Such frequencies could introduce spurious peaks in the FT as both the Fourier analysis and the prewhitening assume constant amplitude. Therefore, we checked for the amplitude and the phase variability of the two highest amplitude periodicities (f_1 and f_2), as we were able to resolve them in each individual run. The peak at 7088.67 μHz appears to vary both in amplitude and in phase. The amplitude and phase of the f_2 mode does not appear to be changing throughout the run. The errors on amplitudes and phases for some runs are too high to allow us to make any claims. All that can be said is that there is a possibility of a periodic change in amplitude and phase for the f_1 frequency with a period of roughly 5 days and that the frequency at f_2 appears to be stable both in amplitude and in phase over the run. Figure 6 shows the behavior of the phase (T_{max}) and amplitude of f_1 and f_2. This figure shows the amplitude and phase of individual long runs; we grouped nearby short runs to reduce the phase and amplitude uncertainties when necessary.

The variability we see in f_1 can be the intrinsic amplitude variability of the mode, or it can be caused by beating of two or more

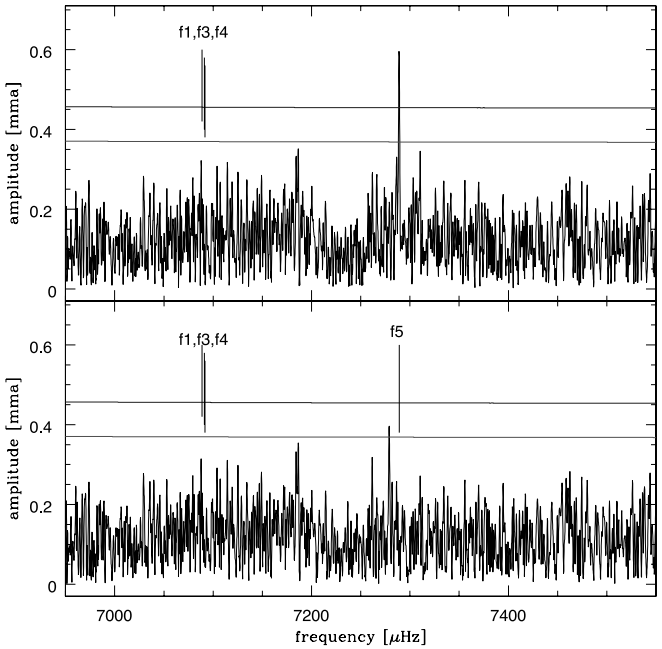

FIG. 7.—*Top:* FT of the entire data set, prewhitened by f_1 to f_4, expanded around f_5. *Bottom:* Residual FT after prewhitening with $f_5 = 7289.0$ μHz. [*See the electronic edition of the Journal for a color version of this figure.*]

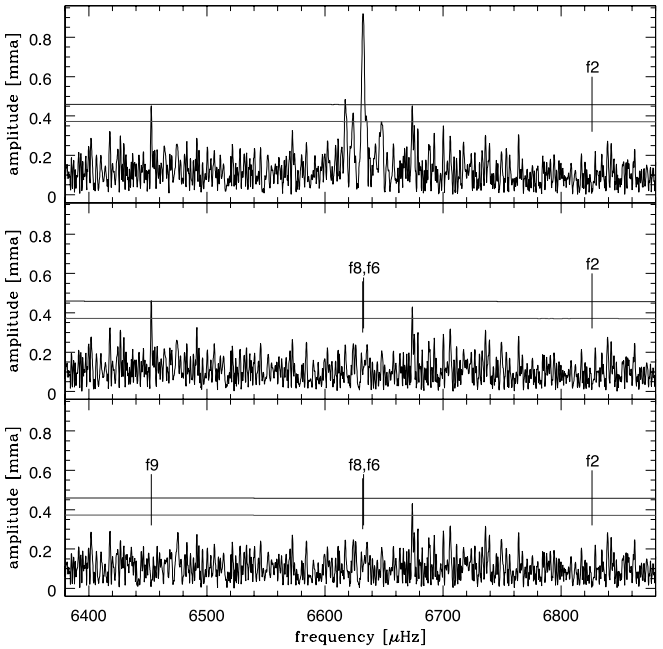

FIG. 8.—*Top:* Residual FT after the first five modes have been removed from the data, in the range from 6380 to 6880 μHz. *Middle:* Temporal spectrum after $f_6 = 6632.8$ μHz and $f_8 = 6631.9$ μHz have also been removed. *Bottom:* FT with additional prewhitening by the $f_9 = 6452.9$ μHz. [*See the electronic edition of the Journal for a color version of this figure.*]

closely spaced frequencies. While the correct answer is impossible to give within the frame of the current time series techniques, all the clues of our analysis point toward attributing the amplitude variability in f_1 to the beating of closely spaced frequencies. If this was a stochastic amplitude variation, the signature in the FT would mimic two or more closely spaced modes of similar amplitude, and complete removal with a single sinusoid in the prewhitening process would not be appropriate. Therefore, the beating of closely spaced frequencies is the most probable cause of the amplitude variability we see in f_1 as it is consistent with the fine structure of two additional closely spaced frequencies we found in the data.

The next highest peak in the FT is at 7289.0 μHz. Figure 7 displays this region of the frequency domain, showing the FT of the data before (*top*) and after (*bottom*) removing this periodicity, with the parameters determined by the NLLS fit to the data. Although there is some power left above the 3 $\sigma_{\rm noise}$ level (lower solid line), NLLS cannot satisfactorily converge on the parameters of these low-amplitude peaks. Hence, prewhitening stops here for this region, but we do list the highest residual peak in this range as a possible real frequency in Table 3.

TABLE 3

MARGINAL DETECTIONS: PEAKS WITH AN AMPLITUDE BETWEEN 3.7 $\sigma_{\rm noise}$ AND 3 $\sigma_{\rm noise}$ SEEN IN WET DATA ON PG 0014+067

Frequency (μHz)	Period (s)	Amplitude (mma)
5921.3	168.882	0.40
6674.0	149.835	0.43
7278.9	137.383	0.40
7895.0	126.662	0.39
7938.3	125.971	0.45
8870.8	112.729	0.42
9576.6	104.421	0.41
9834.2	101.686	0.38
10807.8	92.526	0.36
11116.5	89.956	0.36
11364.8	87.991	0.36
12083.7	82.756	0.37
13539.8	73.856	0.38

Figure 8 shows the region of the next highest power; the top panel shows the residual FT after the five highest peaks have been removed (f_1–f_5). The highest power (amplitude) peak on the upper plot appears as a single peak of about 0.9 mma. Detailed NLLS analysis finds two closely spaced modes at $f_6 = 6632.8$ μHz with an amplitude of 0.65 mma and $f_8 = 6631.9$ μHz with an amplitude of 0.5 mma. After those two sinusoids have been removed from the light curve, the residual spectrum stays clean, as it is shown on the middle panel of Figure 8. The frequency difference between those two modes is of order our resolution, 0.9 μHz. The next highest peak is at $f_9 = 6452.9$ μHz with an amplitude just above our threshold (0.4 mma). Removal of this frequency reveals no more power above the noise (Fig. 8, *bottom*). The only power left in this region is at 6674 μHz but at an amplitude that is below our adopted threshold, albeit above the 3 $\sigma_{\rm noise}$ level. We cannot confirm this frequency is real; we do however indicate this frequency in our "almost" list (Table 3).

At the low-frequency end, there is power with a rather low amplitude, at about 5923 μHz. Just by comparing with the spectral window (Fig. 3), it is clear that we are most probably dealing with two or more closely spaced frequencies. NLLS finds a mode with an amplitude of 0.5 mma at $f_7 = 5923.4$ μHz. Figure 9 shows this region, giving the temporal spectrum before (*top*) and after this mode is removed by prewhitening (*bottom*). There is still excess power left after its removal, with a frequency of 5921.3 μHz. NLLS is unable to converge on a simultaneous fit to these two modes along with the nine found previously. This second frequency is included in the list of possible true periodicities (Table 3).

The only power left above the threshold is just below 6200 μHz. The attempt to find the NLLS fit to the data including this mode

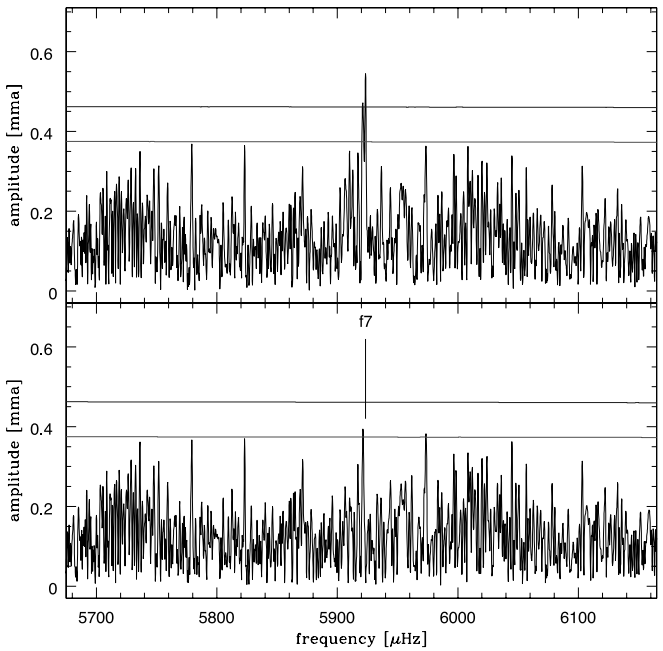

FIG. 9.—Residual FT of the entire data set at the low-frequency end of the main power (*top*) after f_1 through f_6, f_8, and f_9 are removed. Removal of f_7 results in the FT shown in the bottom frame. [*See the electronic edition of the Journal for a color version of this figure*.]

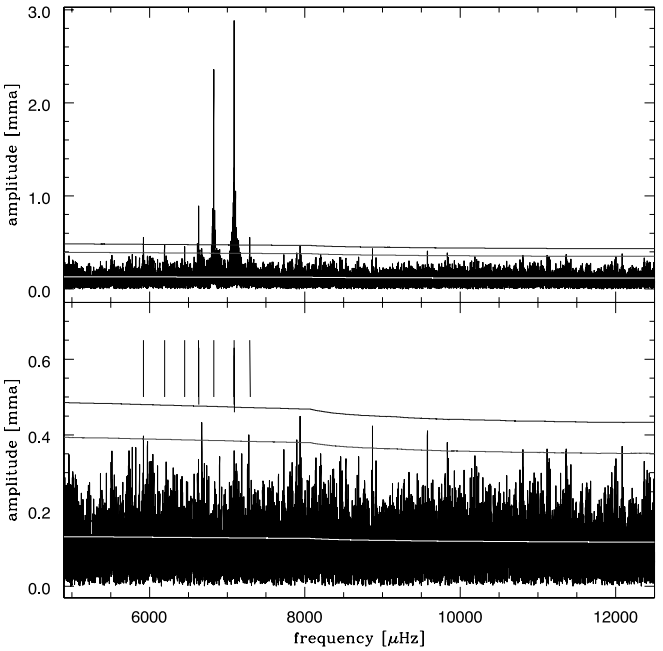

FIG. 11.—Total FT of the original WET data set on PG 0014+067 (*top*) followed by the residual FT of the same data set, prewhitened by the 10 frequencies listed in Table 2. Note that the middle solid line corresponds to 3 $\sigma_{\rm noise}$, while the upper solid line corresponds to 3.7 $\sigma_{\rm noise}$. The white solid line is $\sigma_{\rm noise}$. [*See the electronic edition of the Journal for a color version of this figure*.]

was successful, despite its low amplitude, and we have therefore removed this peak with a frequency of $f_{10} = 6193.5$ μHz and an amplitude of 0.4 mma from the total light curve. Prewhitening successfully removes all the excess power with only the noise left in that region. Figure 10 shows the FT of the residuals. The top panel shows the starting spectrum, in this case the residual FT prewhitened by the nine frequencies found, and the bottom is the FT after we have removed the 10 frequencies.

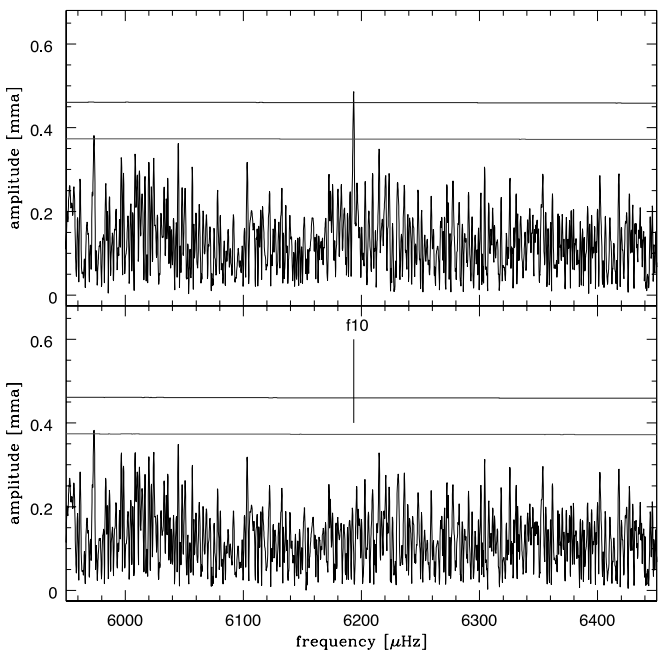

FIG. 10.—FT near f_{10} prewhitened by the nine frequencies f_1 to f_9 (*top*) followed by residual FT after removing the tenth frequency f_{10} (*bottom*). [*See the electronic edition of the Journal for a color version of this figure*.]

To summarize, performing Fourier analysis and NLLS fitting on the entire WET data set obtained during Xcov24, we have detected a total of 10 frequencies in the power spectrum of PG 0014+067 with a 99% significance level and with a resolution of 0.9 μHz. The final results of a simultaneous multiple sin wave fit to the total light curve are summarized in Table 2, listing the frequencies, amplitudes, and phases of the main modes detected in the WET data set. The first column, Mode, gives the name of each frequency as f_n, where n is ordered by relative amplitude. The last column, $T_{\rm max}$, is the time of the first maximum after 2004 August 21 0 hr UT, given in seconds. The uncertainties for the values given in the table are formal least-square estimates of the 1 σ errors.

Figure 11 shows the FT of the combined WET data set on PG 0014+067 before (*top*) and after the removal (*bottom*) of 10 periodicities listed in Table 2. We note that in the region where most peaks appear, the 3.7 $\sigma_{\rm noise}$ level corresponds to about 0.44 mma. There are 13 low-amplitude peaks below our adopted threshold (3.7 $\sigma_{\rm noise}$), albeit above the somewhat less conservative acceptance criterion at 3 $\sigma_{\rm noise}$. One of these, at 13,540 μHz, lies outside of the range displayed in Figure 11. These peaks are at best marginal detections. In Table 3 we list the frequencies, corresponding periods, and amplitudes of those 13 marginally detected modes should they be detected in other data sets.

3.2. *Comparing with Previous Data on PG 0014+067*

In partial support of the run, six nights of observation of PG 0014+067 took place two months prior to Xcov24 (2004 August) using the high-speed multichannel photometer ULTRACAM (Dhillon & Marsh 2001) on the 4.2 m William Herschel Telescope at La Palma (Jeffery et al. 2005). We compare our results with published results on PG 0014+067 from Brassard et al. (2001) and Jeffery et al. (2005). Table 4 lists the periodicities identified by Jeffery et al. (2005) and Brassard et al. (2001) together with the WET results.

TABLE 4
WET Frequencies in PG 0014+067 (in μHz) Compared with the ULTRACAM data (Jeffery et al. 2005) and CFHT Data (Brassard et al. 2001)

Mode	WET	ULTRACAM	CFHT
...	...	5780.9[a]	...
...	...	...	5896.2
f_7	5923.4	5921.9[b]	5923.2
...	...	5924.8	...
f_{10}	6193.5	...	6227.7 = f_{10} + 3 day^{-1}
f_9	6452.9	6454.4	...
f_8	6631.9	...	6630.7
f_6	6632.8	6632.6	6621.1 = f_6 − 1 day^{-1}
...	...	6646.5	...
...	...	6659.9[a]	...
...	...	6726.8[a]	...
f_2	6826.06	6826.1	6837.5 = f_2+1 day^{-1}
...	...	7076.6[a] = f_1 − 1 day^{-1}	7079.1 = f_3 − 1 day^{-1}
f_1	7088.67	7089.1[b]	7088.7
f_3	7091.0	...	...
f_4	7091.7	7091.67[c]	...
...	...	7093.4	...
...	...	7094.8	...
...	...	...	7150.2
...	...	7187.5	...
f_5	7289.0	...	7286.2
...	...	...	7670.3
...	...	...	7952.1
...	...	...	8552.1
...	...	8588.9[a]	...
...	...	...	9797.6
...	...	9971.5	9970.3
...	...	11547.9	...
(2 × f_{10})	...	...	12386.8
(2 × f_9)[d]	...	12910.9[a]	...

[a] Seen in white light only.
[b] Multiplet.
[c] The highest amplitude seen in ULTRACAM data.
[d] Frequency f_9 as seen in ULTRACAM data.

Note that all frequencies identified by the WET (Table 2) were identified by either Jeffery et al. (2005) or by Brassard et al. (2001) or by both to within the cycle per day aliases. The highest amplitude frequency in the WET data is at 7088.67 μHz, and it is seen as a multiplet of three closely spaced frequencies (along with 7091.0 and 7091.7 μHz). The ULTRACAM data set identified four closely spaced frequencies in this range (see Table 4), out of which the highest amplitude one in their data set is at 7091.7 μHz. This multiplet is not identified in the CFHT data, probably due to the resolution of their run; only one frequency of this multiplet is found at 7088.7 μHz. The amplitude and phase of the highest amplitude mode (7088.67 μHz) in the WET data set, as well as the highest amplitude mode (7091.7 μHz) in the ULTRACAM data set, were noticed to vary on the same timescale of 5 days.

The amplitudes of the individual modes in sdBV stars are known to change on the timescale of years, months, and even days (Kilkenny et al. 1999), although the question whether this results from true physical change in the star or beating between closely spaced frequencies still remains unanswered. In this particular case both the WET and ULTRACAM data sets find the amplitude and phase variability on the same timescale and identify closely spaced frequencies, a multiplet around 7090 μHz. This gives an additional credibility to the hypothesis that this relative amplitude change is caused by beating, although longer runs would be needed to confirm this speculation.

4. DISCUSSION

The frequencies we saw in PG 0014+067 during the 2004 October WET campaign showed no obvious patterns that could readily be attributed to rotational splitting or other common effects in nonradially pulsating stars. However, some unusual systematics among the frequencies became readily apparent. In this section we discuss those systematics and explore the statistical significance of such patterns by including additional secure frequencies seen by Jeffery et al. (2005).

4.1. *Strange Systematics in the Observed Frequencies*

The frequency list of PG 0014+067 displays some suggestive systematics. As an exercise in numerology but one that will eventually provide some statistically significant results, we examined these systematics further.

Considering only the dominant modes in each closely spaced multiplet, there are seven main frequencies in the WET data on PG 0014+067, represented by $f_1, f_2, f_5, f_6, f_7, f_9$, and f_{10}. Within this group, we find several pairs of frequencies separated by multiples of 90 μHz. The first six lines in Table 5 list these differences. While not all entries in the table are independent, it illustrates that some (large) frequency differences are very similar to one another, and all share a common factor of 90.47 ± 0.53 μHz.

The frequency f_5 does not pair with any other mode in a difference that is a factor of 90.47 μHz. However, the average value of f_5 and f_1, 7188.8 μHz, is 4 times that interval from f_2. This somewhat suspicious additional entry in Table 5 is supported by the observation of a frequency that lies within 1.3 μHz of that value by Jeffery et al. (2005; the frequency of 7187.5 μHz in Table 4). Thus, the three frequencies ($f_5 = 7289.0$, 7187.5, and $f_1 = 7088.7$ μHz) form a nearly equally spaced triplet with a spacing of about 101.5 μHz. In light of this, we explored the frequencies in Table 2 allowing for an ≈101 μHz deviation; these are shown in the last four lines of Table 5. With this additional complication, additional evidence for a possible chain of frequencies separated by about 90 μHz appears. If we adopt a value of 90.47 μHz for the first spacing, then the last four lines of Table 5 suggest that the second spacing is 101.1 ± 1.4 μHz.

We recognize that the spacings identified by this subjective technique alone may not be unique or even meaningful. We note that there is neither an a priori expectation of a chain of equally spaced (in frequency) modes for these stars nor is there an expectation, based on the physics of the star, for a splitting as large

TABLE 5
Frequency Differences in the PG 0014+067 WET Data

Frequency Pair	Difference (μHz)	Multiple (μHz)
f_6-f_9	179.9	= 2 × 89.95
$f_{10}-f_7$	270.1	= 3 × 90.03
f_1-f_6	455.9	= 5 × 91.17
f_2-f_{10}	632.6	= 7 × 90.37
f_1-f_9	635.8	= 7 × 90.82
$\langle f_5, f_1\rangle-f_2$	362.8	= 4 × 90.69
		Mean spacing = 90.47 ± 0.53
f_5-f_1	200.3	= 2 × 100.15
f_1-f_2	262.6	= 4 × 90.47[a] − 99.29
f_5-f_2	462.9	= 4 × 90.47[a] + 101.01
f_9-f_{10}	259.4	= 4 × 90.47[a] − 102.49
f_2-f_9	373.2	= 3 × 90.47[a] + 101.78
		Mean spacing = 101.1 ± 1.4

[a] Fixed at mean value from lines 1–5.

TABLE 6
PULSATION FREQUENCIES IN PG 0014+067, ALONG WITH AN EMPIRICAL MODEL FIT

Number	Frequency (μHz)	Amplitude (mma)	Note	i	j	Model (μHz)	Difference (μHz)
[a]	5780.9	0.35	ULTRACAM (w)	...	...	...	...
f_7	5923.4	0.54	Fine structure	0	0	5923.2	0.2
f_{10}	6193.5	0.44		3	0	6194.1	−0.6
f_9	6452.9	0.45		7	−1	6454.1	−1.2
f_6 (f_8)	6632.8	0.65	Fine structure	9	−1	6634.6	−1.8
[a]	6646.5	0.60	ULTRACAM	8	0	6645.6	0.9
[a]	6659.9	0.34	ULTRACAM (w)	7	1	6656.5	−3.4
[a]	6726.8	0.37	ULTRACAM (w)	10	−1	6724.9	1.9
f_2	6826.1	2.38		10	0	6826.1	0.0
f_1 (f_3, f_4)	7088.7	2.98	Fine structure	14	−1	7086.1	2.6
[a]	7187.5	0.66	ULTRACAM	14	0	7187.3	0.2
f_5	7289.0	0.65		14	1	7288.5	0.5

[a] No number assigned.

as 101 μHz. Neither 90 nor 100 μHz spacings are seen in theoretical models of these stars. The asymptotic frequency spacing for p-modes in these stars (i.e., modes with $n > l$, consecutive n, and alternating l) is roughly 750 μHz. This value was determined using the model frequencies from Brassard et al. (2001) along with our own sdB models with appropriate values for log g and $T_{\rm eff}$.

Even so, could the 101 μHz splitting be a rotational splitting? While this large splitting could be caused by rotation, the implied rotation rate (if solid-body rotation), although not ruled out, would be faster than any known single sdBV detected so far, based on spectroscopic study of line profiles. Spacings this large are seen only in close binary pulsating sdBV stars such as PG 1336−018 (Kilkenny 2003). On the other hand, Kawaler & Hostler (2005) suggest that rapid internal rotation could produce large splittings in a star with a slow surface rotation rate, but their predictions suggest that the splittings of modes differing in n and l should not show the same value.

4.2. *An Empirical, Phenomenological Relation*

With two apparent splittings present, we decided to explore an entirely phenomenological parameterization that could then be used to make an empirical fit to the observed frequencies and provide a framework for determining the statistical significance of these patterns. We chose a form reminiscent of asymptotic p-mode pulsation with a constant rotation frequency

$$f(i,j) = f_0 + i\delta + j\Delta, \quad (1)$$

where δ represents a small spacing (and i is an integer ranging from 0 upward) and Δ represents a large spacing (with j initially limited to being either -1, 0, or 1). In the equation above, f_0 represents a zero point for the fit with $i = j = 0$.

In the general case of fitting an observed set of frequencies, we performed a two-dimensional χ^2 minimization over a grid of values of δ from 40 to 120 μHz and Δ from 80 to 210 μHz. For each (δ, Δ) pair, we found the combination of (i, j) that minimized the rms difference between the observed and model frequencies and computed the χ^2 of the fit. Clearly, there is an aliasing problem when the combinations of i, j, δ, and Δ produce commensurate spacings, so the χ^2 surface shows multiple minima. To help break that degeneracy, we impose an additional criterion that a (δ, Δ) solution result in at least two modes that have the same value of i but different j. The quantized nature of the problem (the values of i and j are constrained to be integers) and the additional constraint on the values of j complicate determination of statistical significance of any fits. Therefore, to find the form of the distribution of χ^2 for a random selection of frequencies, we performed a series of Monte Carlo trials using frequency lists drawn from uniformly random distributions within the range shown by PG 0014+067.

Using only the WET frequencies, we find two solutions of high significance; however, only one satisfies the requirement of having two modes with the same value of i but different values of j. That solution is the one found by the successive differencing procedure described in the previous subsection. The fit values were $\delta = 90.37$ μHz, $\Delta = 101.46$ μHz, and $f_0 = 5922.46$ μHz.

With only seven frequencies and more than three free parameters (the values of δ, Δ, and f_0 are free, but the choices of i and j are constrained), the fit above is not well constrained. Via the Monte Carlo technique with seven frequencies, we find the fit to be significant at the 95% confidence level; that is, in a trial of 285 frequency sets, only 13 had a lower value of χ^2 and at least two modes with the same value of i and different values of j. While this is encouraging in terms of suspecting that the parameterization above may be meaningful, it is not, by itself, very convincing.

Fortunately, we have additional frequencies in this star that have been reliably measured by others that lie within the frequency range from the WET data alone. This list is given in Table 6. By "reliable" we mean peaks seen in more than one investigation and those that are clearly true peaks and not aliases. Given the exceptional quality and clean window of the ULTRACAM data, we give that data set higher relative weight, using the WET to resolve residual ambiguities originating from diurnal aliases. Using these additional observations, five additional frequencies in the range in which the WET showed pulsations can be examined for compliance with the relation derived using only the seven WET frequencies in Table 4.

Of the five additional frequencies in Table 6, four fit the pattern determined from the WET frequencies alone *using the same parameters*. Again, we use Monte Carlo simulations of this process to judge whether or not this is a significant effect. In this case we measure the rms deviation of five additional randomly chosen frequencies from the previously established relation from the WET data. The rms deviation is calculated after dropping the worst fitting of the five. Comparing the distribution of the rms deviations in the Monte Carlo trials with that from the data in Table 6 reveals that the fit of the relation (eq. [1]) with the data is significant at the 99.4% confidence level (based on 9829 trials) under these conditions.

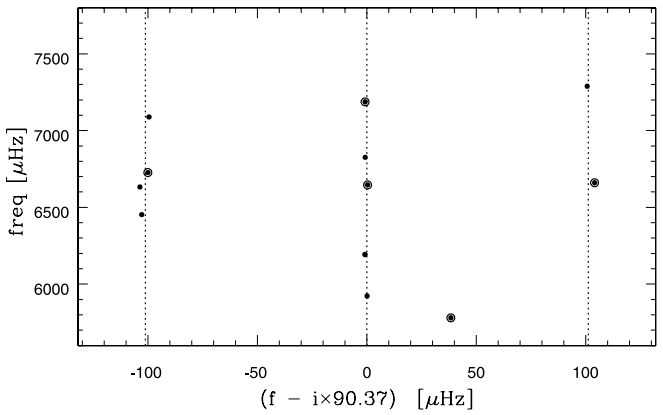

FIG. 12.— "Echelle" diagram of the frequencies in PG 0014+067. The frequencies have been folded on the small spacing $\delta = 90.37$ and stacked, showing the uniformity of the frequency spacings within the main band and the two side bands separated from the main band by the large spacing $\Delta = 101.22$ μHz. Expanded points are from the non-WET modes in Table 6.

In practice, we impose an additional requirement that the fit must include modes that have at least two pairs with the same i but different j (i.e., that at least two values of i show more than one j component). Enforcing this additional condition on the fit criteria restricts the aliasing problem and results in a smaller number of possible solutions. This process also results in a much higher statistical significance for the fit to PG 0014+067; the confidence level rises to the 99.95% level. In the fit in Table 6, we see that there are three values of i that have more than one j component, with one complete "triplet," a concordance that none of the 9829 Monte Carlo trials reached.

Finally, we can employ the fit procedure using all of the modes in Table 6 to determine more accurate values of the parameters of equation (1). For PG 0014+067 this procedure yields values of $\delta = 90.37$, $\Delta = 101.22$, and $f_0 = 5923.24$ (all in microhertz). Using these values in equation (1), we find the model frequencies listed in Table 6. Note that the fit is extremely good; all but 1 of the 12 modes identified in the table are fit to within 0.05%, with an rms difference of 0.013δ. To illustrate the closeness of the fit, Figure 12 shows the frequencies of PG 0014+067 in an "echelle diagram" similar to those used in helioseismology. The vertical axis is frequency, and the horizontal axis (also in frequency units) shows the departure of each mode from an integral multiple of the small spacing δ. The repeating pattern of $j = 0$ modes stacks above an ordinate of 0, while modes with nonzero values of j lie on either side at frequencies Δ away.

Is this asymptotic pulsation? After all, high-order p-modes show a more-or-less constant frequency spacing; such sequences are seen in helioseismic data and in the rapidly oscillating Ap stars (i.e., Kurtz et al. 2005). The sequence of modes split by integral multiples of δ cannot be asymptotic p-mode behavior. As mentioned above, models of PG 0014+067, and sdBV pulsators in general, indicate that the radial fundamental frequency in the models is usually close (in frequency) to the observed mode frequencies. Asymptotic relations such as equation (1) are usually valid (at the few percent level) only for values of $n \gg l$, or more generally for large values of n. Even so, the computed frequency separation for p-modes in sdBV models yields values of several hundred microhertz, a factor of 5 or more larger than what PG 0014+067 shows.

In summary, the frequencies seen in PG 0014+067 obey a simple empirical trend, one that cannot be understood in terms of standard evolutionary and pulsation models for such stars. Simply put, there is no applicable physics in this purely empirical fit. In a subsequent paper, we will examine the frequencies present in other well-studied sdB stars, and we show that they show a similar pattern as well. The theoretical interpretation of this pattern is not at all clear, but we anticipate that the systematic frequency differences discovered in PG 0014+067 and other sdB stars could be a very important clue to unlocking some secrets of their interiors.

Financial support for this work came from the US National Science Foundation (NSF), through grant AST20205983 to Iowa State University. As of 2005 September 1, M. V. is a Ph.D. student of the Research Council of the Katholieke Universiteit Leuven under the doctoral scholarship OE/05/20. She acknowledges additional financial support from Katholieke Universiteit Leuven grant GOA/2003/04. M. V. would like to thank Elizabeth Potter and Chris Tourek for helping the Xcov24 headquarters and with the data reduction. Z. C. and M. P. acknowledge financial support from Hungarian OTKA T-038440 and T-046207. NSF grant AST 03-7480 to Missouri State University supported traveling costs and the camera used by M. D. R. S. J. O. T. is supported by the Deutsches Zentrum fr Luft- und Raumfahrt (DLR) through grant 50-OR-0202.

REFERENCES

Brassard, P., Fontaine, G., Billeres, M., Charpinet, S., Liebert, J., & Saffer, R. A. 2001, ApJ, 563, 1013
Charpinet, S., Fontaine, G., & Brassard, P. 2000, ApJS, 131, 223
Charpinet, S., Fontaine, G., Brassard, P., Green, E. M., & Chayer, P. 2005, A&A, 437, 575
D'Cruz, N. L., Dorman, B., Rood, R. T., & O'Connell, R. W. 1996, ApJ, 466, 359
Dhillon, V., & Marsh, T. 2001, NewA Rev., 45, 91
Dorman, B., Rood, R. T., & O'Connell, R. W. 1993, ApJ, 419, 596
Fusi Pecci, F., & Renzini, A. 1976, A&A, 46, 447
Han, Z., Podsiadlowski, Ph., Maxted, P. F. L., & Marsh, T. R. 2003, MNRAS, 341, 669
Han, Z., Podsiadlowski, Ph., Maxted, P. F. L., Marsh, T. R., & Ivanova, N. 2002, MNRAS, 336, 449
Handler, G., 2003, Baltic Astron., 12, 253
Iben, I. 1990, ApJ, 353, 215
Jeffery, C. S., et al. 2005, MNRAS, 362, 66
Kawaler, S. D. 1999, in ASP Conf. Ser. 169, Procedings of the 11th European Workshop on White Dwarfs, ed. J. E. Solheim & E. Meištas (San Francisco: ASP), 158
Kawaler, S. D., & Hostler, S. 2005, ApJ, 621, 432
Kilkenny, D. 2002, in IAU Colloq. 185, Radial and Nonradial Pulsations as Probes of Stellar Physics, ed. C. Aerts, T. R. Bedding, & J. Christensen-Dalsgaard (ASP Conf. Ser. 259; San Francisco: ASP), 356
Kilkenny, D., Koen, C., O'Donoghue, D., & Strobie, R. S. 1997, MNRAS, 285, 640
Kilkenny, D., et al. 1999, MNRAS, 303, 525
———. 2003, MNRAS, 345, 834
Kleinman, S. J., Nather, R. E., & Philips, T. 1996, PASP, 108, 356
Kurtz, D. W., et al. 2005, MNRAS, 358, 651
Kuschnig, R., Weiss, W. W., Gruber, R., Bely, P. Y., & Jenkner, H. 1997, A&A, 328, 544
Metcalfe, T. S., Nather, R. E., Watson, T. K., Kim, S.-L., Park, B.-G., & Handler, G. 2005, A&A, 435, 649
Mengel, J. G., Norris, J., & Gross, P. G. 1976, ApJ, 204, 488
Poindexter, S., et al. 2003, AAS Meeting, 203, 12.16
Riddle, R., 2003, Baltic Astron., 12, 183